# A hybrid method towards automated nipple detection in 3D breast ultrasound images

Lei Wang [1] Tobias Böhler [1] Fabian Zöhrer [1] Joachim Georgii [1] Claudia Rauh [2] Peter A. Fasching [2] Barbara Brehm [3] Rüdiger Schulz-Wendtland [3] Matthias W. Beckmann [2] Michael Uder [3] Horst K. Hahn [1]

***Abstract*— In clinical work-up of breast cancer, nipple position is an important marker to locate lesions. Moreover, it serves as an effective landmark to register a 3D automated breast ultrasound (ABUS) images to other imaging modalities, e.g., X-ray mammography, tomosynthesis or magnetic resonance imaging (MRI). However, the presence of speckle noises caused by the interference waves and variant imaging directions poses challenges to automatically identify nipple positions. In this work, a hybrid fully automatic method to detect nipple positions in ABUS images is presented. The method extends the multi-scale Laplacian-based method that we proposed previously, by integrating a specially designed Hessian-based method to locate the shadow area beneath the nipple and areola. Subsequently, the likelihood maps of nipple positions generated by both methods are combined to build a joint-likelihood map, where the final nipple position is extracted. To validate the efficiency and robustness, the extended hybrid method was tested on 926 ABUS images, resulting in a distance error of $7.08 \pm 10.96$ mm (*mean* $\pm$ *standard deviation*).**

## I. INTRODUCTION

Mammography suffers poor sensitivity in screening patients with dense breasts. In complement to mammography, automated 3D breast ultrasound (ABUS) emerges as an important tool in breast cancer diagnosis. Recent studies reported that supplemental ABUS increases detection rate of small and mammography occult breast cancers [1], [2]. In computer-aided diagnosis (CAD), interpretation of ABUS data has gained significant interests [3], [4]. In a CAD system, as an important reference marker, nipple position allows for localizing the quadrants of breast lesions. Furthermore, fusion of ABUS data with other imaging modalities, such as mammography, MRI or tomosynthesis, nipple positions provides stable spatial correlation and are used to improve registration accuracy. In this work, a hybrid fully automatic method to detect nipple positions in ABUS images is presented. The method extends the multi-scale Laplacian-base method that we proposed previously [5], by integrating a specially designed Hessian-based method to locate the shadow area beneath the nipple and areola.

## II. MATERIALS AND METHODS

### A. Dataset

Compared with our previous study [5], we enhanced the data set with more collected scans, including 926 ABUS image sequences acquired by Siemens S2000 ABVS systems as part of the iMODE-B (imaging and molecular detection for breast cancers) study at the University Breast Center Franconia, University Hospital Erlangen, Germany. The study was approved by the Ethics Committee of the Medical Faculty, Friedrich-Alexander University Erlangen Nuremberg and all patients gave written informed consent. Breasts were scanned in five possible imaging views: anterior-posterior (AP), medial (MED), lateral (LAT), superior (SUP) and inferior (INF) (as shown in Fig. 1). Acquisitions in different views involve different compressions of breasts, which leads to variant imaging characteristics of nipples. The presence of nipples varies according to different acquisition views. The locations of nipples were clearly identified in AP views and distributed in peripheral regions in other views. For several extreme cases where the nipples were pushed to the image borders, a portion of the nipples were still visible. The in-plane image resolution of the collected ABUS volumes is $719 \times 565$ with a slice number of $\times 318$, associated with in-plane voxel spacing of $0.2 \times 0.07$ mm and slice thickness of 0.525 mm. To validate the performance of our method, an experienced radiologist annotated all images by pinpointing the tip points of nipples (a tip point is the most anterior point of a nipple in coronal planes), serving as the ground truth.

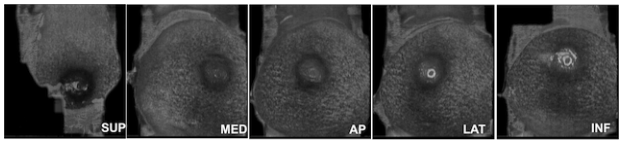


Fig. 1. ABUS scans for the left breast of a patient, illustrating nipple positions in different imaging views: AP, MED, LAT, SUP and INF.

## III. METHODS

The hybrid method combines the detection power of both Hessian detector and Laplacian detector. The tube-like shadow observed beneath nipple and areola in ABUS data inspires the idea of applying a 3D Hessian-based tubular filter to enhance the shadowing region, resulting a Hessian-based likelihood map. Meanwhile, the multi-scale Laplacian blob detector builds a Laplacian-based likelihood map. Multiplying these two maps ends up with a joint probability distribution of nipple position, where the most probable nipple position can be estimated. A schematic overview of the proposed hybrid method is given in Fig. 2.

[1]Fraunhofer MEVIS - Institute for Medical Image Computing, Bremen, Germany lei.wang@mevis.fraunhofer.de

[2]Frauenklinik des Universitätsklinikums Erlangen, Germany

[3]Institut für Diagnostische Radiologie des Universitätsklinikums Erlangen, Germany

978-1-4244-7929-0/14/$26.00 ©2014 IEEE

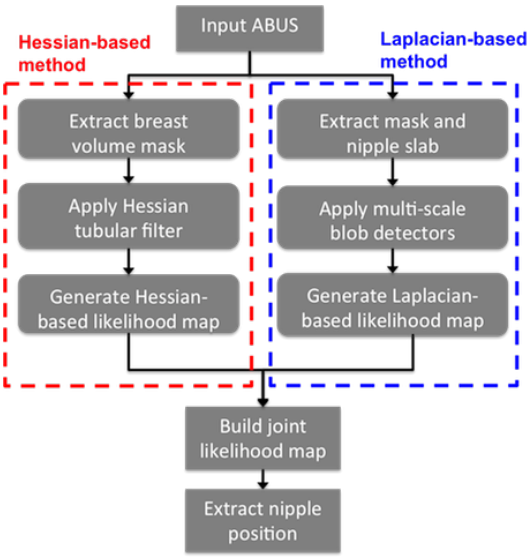


Fig. 2. Schematic workflow of the hybrid detection method

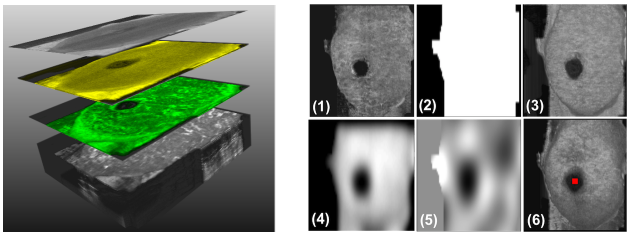


(a) (b)

Fig. 3. (a) 3D visualization of the extracted nipple slab (yellow) and mask slab (green). (b) workflow of blob structure detection: (1) MinIP image of the mask slab; (2) generated binary mask; (3) MaxIP image of the nipple slab; (4) down-sampled and smoothed MaxIP image; (5) response of LoG filter at scale $\sigma = 6$; (6) extracted global minima and detected nipple position (red).

### A. Multi-scale Laplacian-based nipple detection

In previous works, we explored a fully automated nipple detection method employing a multi-scale Laplacian-based blob detector [5]. The method is comprised of several pre-processing steps to find the region of interest (ROI) of the nipple and build a binary mask that excludes background. Then, a multi-scale blob detector is employed to detect the nipple tip point.

*1) Pre-processing:* In pre-processing step, all images were reformatted to coronal planes. Noticing that nipple always appears in a bunch of anterior coronal slices near to transducer, a nipple slab with the thickness of 1.5 mm enclosing a pile of anterior coronal slices is extracted, starting with the slice with a distance of 0.35 mm to the transducer panel. The nipple slab defines a ROI, where subsequent nipple detection algorithms are applied to localize nipple tip points. In addition, to remove background, a mask slab with the same thickness of 1.5 mm following the nipple slab is extracted (see Fig. 3(a)). Then, the minimum intensity projection (MinIP) image over all slices of the mask slab is calculated, resulting in a 2D projected image where the intensities of background areas are almost zero (Fig. 3(b)(1)). By a simple thresholding process, a binary mask is obtained. Followed by a morphological closing operation with a kernel size $5 \times 5$, holes and gaps of the binary mask are filled (Fig. 3(b)(2)). Similarly, the maximum intensity projection (MaxIP) image of the nipple slab is computed, resulting in a 2D map, in which the nipple tip point will be searched for (Fig. 3(b)(3)). To reduce computational expense, the MaxIP image of the nipple slab and the mask image are down-sampled to a lower in-plane resolution defined by a fixed scale factor: $0.125 \times 0.125$. To eliminate disturbing structures, the MaxIP image is further smoothed by a Gaussian kernel with $\sigma = 3$ (Fig. 3(b)(4)).

*2) Blob detection:* A key observation is that the nipple appears as a 2D dark blob structure in the MaxIP image of the nipple slab, which can be enhanced by a commonly used blob descriptor: Laplacian of Gaussian filter (LoG) [6]. Given a MaxIP image $I(x,y)$ and a Gaussian kernel at scale $\sigma$: $g(x,y,\sigma)$, the MaxIP image convolved with multiple Gaussian kernels with variant sizes leads to a scale-space representation: $L(x,y,\sigma) = I(x,y) \star g(x,y,\sigma)$ [7]. The Laplacian operator $\nabla^2 L = L_{xx} + L_{yy}$ is then calculated at each scale $\sigma$, which produces strong negative response in dark blob regions (Fig. 3(b)(5)). We adopted a multi-scale LoG filter with variant $\sigma$ ranging from 1.5 to 15 mm with a step size of 1.5 mm. The optimal scale that delivers the global minimal response is selected, and the corresponding 2D coordinate in the MaxIP image is recorded as the nipple position in $X$ and $Y$ dimensions. To fetch the $Z$ dimension, we projected the 2D point back to the middle slice of the nipple slab, which reconstructs the 3D position of the nipple (Fig. 3(b)(6)).

### B. Hessian-based nipple detection

Due to the acoustic properties of the nipple and areola, the strength (amplitude) of echo signals received from tissues beneath nipple and areola is normally weak. Hence, a tube-like structured shadow beam is formulated beneath the nipple and areola. Normally, the shadow beam attached to the nipple and areola starts from the first several anterior slices and extends to the posterior slices in coronal view (see Fig. 4). In comparison to other dark regions with variant lengths and shapes originated by other tissues and lesions, it almost traverses through the breast and reaches to chest wall. Based on these observations, a Hessian-based tubular filter is designed to locate the nipple shadow beam, from which the corresponding nipple position can be identified.

Hessian-based filters have been widely employed to analyze local structures of 3D images. Eigen values of the Hessian matrix present different patterns for various geometrical structures, such as blob-like, tube-like or sheet-like objects [8]. Assuming the Eigen values ordered in $\lambda_1 \geq \lambda_2 \geq \lambda_3$, a dark tube-like structure conforms to a pattern of $\lambda_3 \approx 0, \lambda_1 \approx \lambda_2 \gg 0$, where the first and second Eigen values are positive and larger than 0 (see Fig. 4). For other geometrical structures, the second Eigen values of sheet-like and noise structures are approximately close to 0, and all the Eigen

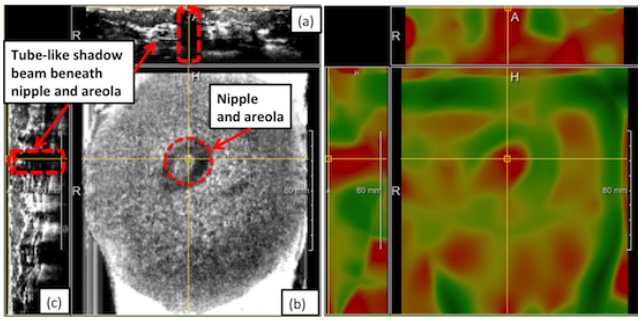


Fig. 4. (Left) Shadow beam beneath nipple and areola in orthogonal views: (a) axial (b) coronal and (c) sagittal; (Right) A heat map visualized the computed second largest Eigen value $\lambda_2$ (red represents larger values)

values of blob-like structures are equally larger than 0 [9].

To exclude background, a mask volume is built by analyzing the intensity histogram of the input ABUS volume. The quantile of $25th$ percent is chosen as the minimal intensity to eliminate background air (see Fig. 5(b)). Then, the Eigen values of each voxel is computed (see Fig. 5(c)). To build a fast and efficient tubular filter to enhance nipple shadow beam, we chose a simplified measure $S$ that accumulates all the second larger Eigen values along the depth direction in coronal view: $S = \Sigma_1^n \lambda_2$ (Fig. 5(d)), where $n$ is the depth dimension. After integral over the depth dimension, a 2D likelihood map scaled between 0 and 1 is built, from which the maxima is extracted which expresses the projected 2D position of the center line of the nipple shadow beam. Ideally, this position represents the nipple position as well, as the center of the nipple correlates with the center line of shadow beam. Finally, the position of the maxima is projected back to the top anterior location which is 0.75 mm to the first coronal slice, and recognized as the final detected 3D nipple position. It is noticed that blob-like structures also yield a larger $\lambda_2$. However, due to the limited amounts and scales of the blob-like structures presented in volumes, they do not produce significant larger accumulation on the likelihood map after integrating over the depth dimension.

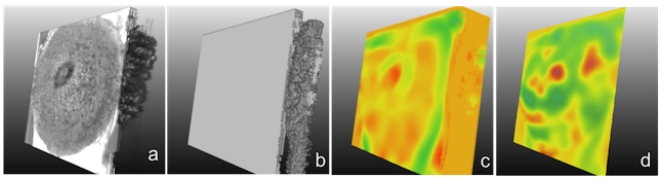


Fig. 5. Workflow illustration of Hessian-based method: (a) a 3D input ABUS volume; (b) the mask volume; (c) the heat map of $\lambda_2$ (red represents larger values); (d) the accumulated response of Hessian tubular filter: $S$.

### C. Hybrid detection method

Both Hessian-based and Laplacian-based method yield two likelihood maps indicating the probability distribution of nipple position. Therefore, it is natural to combine them to estimate a hybrid joint distribution, which is potentially able to improve detection accuracy. Since the original Laplacian response conveys negative values to the dark blob region, the sign of its value is inverted. Then, both response images are scaled in the range of $[0,1]$ to estimate probability distribution (Fig. 6(a,b)). Eventually, the two likelihood maps are multiplied, resulting in a joint map (Fig. 6(c)), where the most probable nipple position is extracted (Fig. 6(d)).

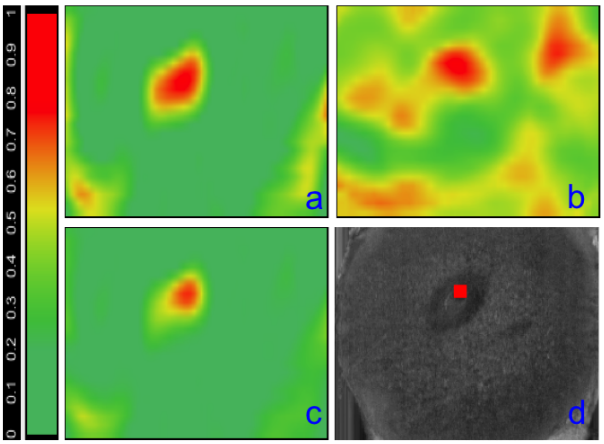


Fig. 6. (a) the likelihood map built by Laplacian method; (b) the likelihood map built by Hessian method; (c) the hybrid likelihood map; (d) the maxima extracted from hybrid map, indicating most probable nipple position.

## IV. Results and Evaluations

The proposed method was tested on 926 healthy and pathological ABUS volumes. The average computation time per ABUS volume was 5 seconds on a machine with a 3.7GHz CPU. The detection accuracy was quantitatively measured by calculating the root-mean-square distance in mm (RMSD) between detected nipple positions and annotated ground truth in 3D. Statistical analysis of the distance error were conducted, obtaining a result of $7.08 \pm 10.96$ mm for the hybrid method. To demonstrate the improvement of combining both methods, the performance of each single method was tested separately, resulting in $8.18 \pm 15.64$ mm for Laplacian-based method and $13.67 \pm 20.73$ mm for Hessian-based method (see Fig. 7). Figure 8 demonstrates the histogram analysis of RMSD, showing the majority of distance errors of all methods fall in the interval of $(0,10)$ mm. The hybrid method outperforms each single methods. Moreover, the distribution of detection rates against variant tolerant thresholds of distance errors is depicted in Fig. 9. It is noticed that hybrid method obtains higher detection rate when tolerant error is larger then than 7 mm. More specifically, when setting tolerance as 10 mm, which is the average size of nipples in our database, nearly 88% of test images were correctly detected by hybrid method, which again exceeds 85% of Laplacian-based method and 74% of Hessian-based method.

By investigating the outliers with large errors, we find that the method might fail when nipples were pushed to image borders during acquisition and imaged partially in extracted nipple slabs. Besides, both the LoG and Hessian filters were proved to perform stably in detecting target nipple position. However, when the breast mask extracted from mask slab is

not sufficiently accurate, or a lesion that mimics the features of the nipple appears in the nipple slab, they might be attracted by spurious structures and recognize them as nipple positions.

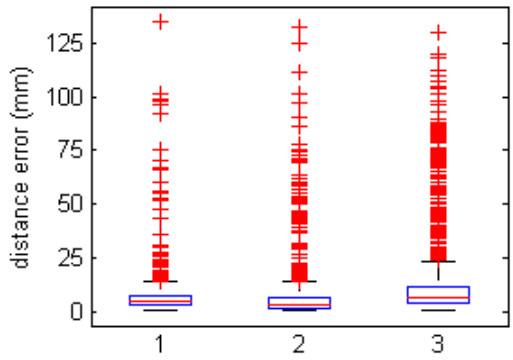


Fig. 7. Boxplot of distance errors associated with hybrid (1), Laplacian-based (2) and Hessian-based (3) methods.

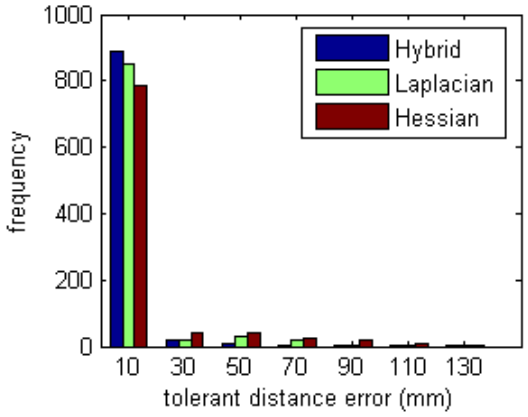


Fig. 8. Histogram distribution of RMSD calculated for each method.

## V. Conclusion and Discussions

In this work, we presented a hybrid method to detect nipple positions in ABUS scans. The Laplacian-based method is designed to detect nipple in an extract nipple slab, using a 2D Laplacian-based blob detector, whereas, Hessian-based method explores the entire ABUS volume and seeks for the location of shadow beam associated with nipple and areola. By combining these two detectors, a joint likelihood map is built, providing more accurate estimation of nipple position. A test on 926 ABUS volumes shows the capability of the hybrid method to precisely detect nipples.

Both Laplacian and Hessian methods are designed under different assumptions: Laplacian method assumes the nipple appears near to transducer and exhibits as a dark blob structure, which could be mimicked by other type of lesions; Hessian method assumes the presence of shadow beam beneath nipple and areola, which is robust against the

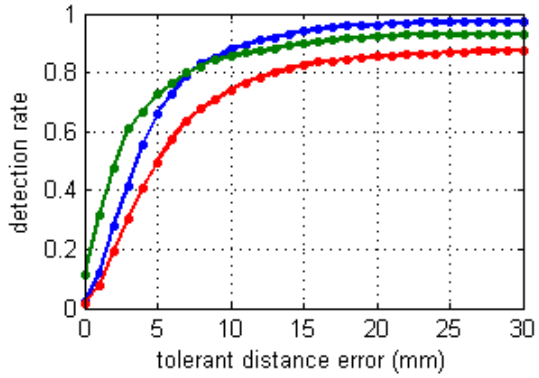


Fig. 9. Detection rates against variant tolerant distance errors drawn for each method.

presence of lesions that normally exhibit weaker shadowing strength than nipple and areola. The idea of combining both methods is inspired by the fact that the hybrid method could overcome the shortcomings of each individual. However, in case the nipple is not sufficiently scanned in the field of view, or the structures, such as lesions, which mimic the properties of nipples, the hybrid method might fail.

## Acknowledgment

This work was supported by the German Federal Ministry of Education and Research (BMBF), project grant No. 13EX1012D. The research leading to these results has received co-funding from the European Unions Seventh Framework Programme FP7 under grant agreement No. 306088.

## References

[1] Giuliano, V., Giuliano, C.: Improved breast cancer detection in asymptomatic women using 3D-automated breast ultrasound in mammographically dense breasts, Clinical imaging, 480-486, (2013)

[2] Nothacker, M., Duda, V., Hahn, M., Warm, M., Degenhardt, F., Madjar, H., Albert, U.-S.: Early detection of breast cancer: benefits and risks of supplemental breast ultrasound in asymptomatic women with mammographically dense breast tissue. A systematic review, BMC cancer, 9, 335, (2013)

[3] Tan, T., Platel, B., Mus, R., Tabar, L., Mann, R. M., Karssemeijer, N.: Computer-aided detection of cancer in automated 3-D breast ultrasound, IEEE transactions on medical imaging, 32(9), 1698-1706, (2013)

[4] Tan T., Platel B., Twellmann T., van Schie G., Mus R., Grivegnee A., Mann R.M., and Karssemeijer N.: Evaluation of the Effect of Computer-Aided Classification of Benign and Malignant Lesions on Reader Performance in Automated Three-dimensional Breast Ultrasound, Academic Radiology, 20, 1381-1388, (2013)

[5] Wang, L., Böhler, T., Zöhrer, F., Georgii, J., Rauh, C., Fasching, P., Brehm, B., Schulz-Wendtland, R., Beckmann, M. W., Uder, M., Hahn, H. K.: Fully Automated Nipple Detection in 3D Breast Ultrasound Images. International Workshop on Breast Imaging, (2014)

[6] Huertas, A. and Medioni, G.,: Detection of intensity changes with sub pixel accuracy using Laplacian-Gaussian masks, IEEE Trans. On Pattern Analysis and Machine Intelligence, 8, 651-664, (1986)

[7] Lindeberg T.: Feature detection with automatic scale selection, International Journal of Computer Vision, 30 (2), 77-116, (1998)

[8] Descoteaux, M., Collins, D. L., Siddiqi, K.: A geometric flow for segmenting vasculature in proton-density weighted MRI. Medical Image Analysis, 12(4), 497-513, (2008)

[9] Frangi, A. F., Niessen, W. J., Vincken, K. L., Viergever, M. A.: Multiscale vessel enhancement filtering. In MICCAI, Vol. 1496, pp. 130-137, (1998)